

MODELING AND SIMULATION OF BIOHEAT POWERED SUBCUTANEOUS THERMOELECTRIC GENERATOR

Ujjwal Verma, Jakob Bernhardt, Dennis Hohlfeld
Institute of Electronic Appliances and Circuits
University of Rostock, Rostock, Germany
Email: dennis.hohlfeld@uni-rostock.de

KEYWORDS

Thermoelectric generator, Seebeck effect, Bioheat, Medical implants.

ABSTRACT

Electrically active implants are gaining interest for an aging European population. The current generation of implants are powered by batteries that have limited lifetime; once depleted they require surgical reinterventions for their replacement. In this paper, we present a multi-physical model of a thermoelectric generator that utilizes the subcutaneous temperature gradient. The gained electrical power can be used to supply an electrically active implant. Furthermore, this paper studies various parameters that influence the temperature gradient. We implemented a simple human tissue model and a more detailed geometry model based on segmented magnetic resonance imaging (MRI) data.

INTRODUCTION

By 2060 every third person in Europe is expected to be more than 65 years old, the subsequent socio-economic impacts lead to an increase in associated medical treatments. Implantable medical devices, more specific electrically active implants, have found success in clinical trials. These are gaining interest especially for treatments like bone tissue regeneration and treating motion disorders using deep brain stimulation (Watkins, Shen and Venkatasubramanian, 2005). All of these implants require electrical power to fulfil their function. Typically, non-rechargeable batteries are used as a source. According to a study (Parsonnet and Cheema, 2003), individuals with pacemakers powered by lithium batteries required a reoperation every 7 or 8 years; most commonly for replacement of the battery.

Many alternative methods have been explored for substituting the lithium batteries, e.g. bio-fuel cells that use glucose as a fuel to power the implant, and nuclear cells for pacemakers, but due to an added risk of radiation poisoning and reliability concerns this is not a viable option (Amar, Kouki and Cao, 2015). While these methods are an improvement in energy autonomy, they still have certain drawbacks such as high cost, possible contamination or inadequate performance, etc. To ensure proper operation, implants need to rely on continuous and sufficient power supply.

Among the various potential energy sources available from the human body, here the thermal gradient between the skin surface and the body core (37 °C) is

investigated at different locations. Thermoelectric generators (TEG) present a viable opportunity for tapping into these sources to provide stable and sufficient power.

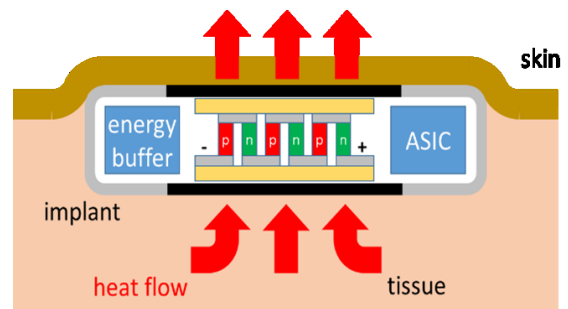


Figure 1: Subcutaneous implant with thermoelectric energy conversion powered by body heat

This paper investigates the energy harvesting potential of a custom TEG compared to commercially available modules. Finally, a possible approach of integrating TEGs into human tissue is presented.

THERMOELECTRIC GENERATOR

Thermoelectric generators are solid-state devices that enable conversion of thermal to electrical energy. Figure 2 shows the setup of a typical TEG. The assembly is made from an array of thermocouples consisting of p-type (hole transporting) and n-type (electron transporting) semiconductor elements. These are connected electrically in series with copper interconnects. The thermocouples are thermally connected in parallel between two ceramic plates.

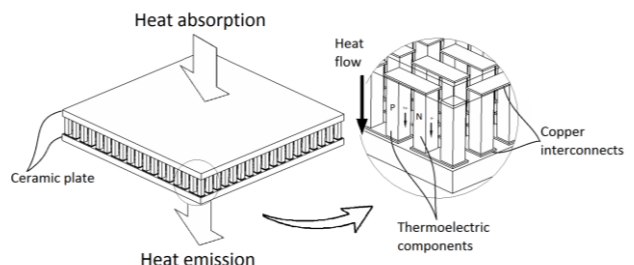


Figure 2: Thermoelectric module with ceramic insulating plates, thermocouples and copper interconnects. A temperature difference generates voltage across the chain of thermocouples

Thermocouple

The energy conversion in a thermocouple is based on the Seebeck effect, which is illustrated in Figure 3, where a temperature difference drives charge carrier diffusion towards lower temperatures. This results in a potential difference across the thermocouple.

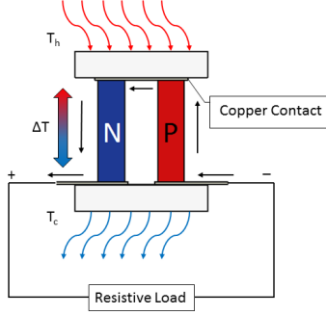


Figure 3: Simplified thermoelectric device with a temperature gradient across the device

The magnitude of the voltage output from equation (1) is proportional to the difference of the Seebeck coefficients α_1 and α_2 , the number of semiconductor thermocouples n and the temperature difference ΔT . The maximum power delivered into a load resistor can be calculated using equation (2) with R_{el} as the internal resistance of the TEG (Strasser et al., 2002).

$$V_{out} = n \cdot \Delta T (\alpha_1 - \alpha_2) \quad (1)$$

$$P_{max} = \frac{V_{out}^2}{4 R_{el}} \quad (2)$$

Figure of Merit

The performance of thermoelectric modules is measured using a dimensionless quantity called figure of merit (ZT) given by equation (3). To obtain a high value, both Seebeck coefficient (α) and electrical conductivity (σ) should be increased, whereas thermal conductivity (κ) shall be minimized. For a thermoelectric device with two semiconductor materials (Tritt, 2002), the figure of merit is calculated using equation (4) where, ρ is the electrical resistivity and the respective material properties of p-type and n-type material are used.

$$ZT = \frac{\sigma \alpha^2 T}{\kappa} \quad (3)$$

$$ZT = \frac{(\alpha_p + \alpha_n)^2 T}{[(\rho_n \kappa_n)^{1/2} + (\rho_p \kappa_p)^{1/2}]^2} \quad (4)$$

Thermoelectric Material Properties

Most commercially available thermoelectric devices use doped semiconductors with large values for the Seebeck coefficients. For room temperature applications bismuth telluride is used with a typical ZT value ranging from 0.8 to 1.0. To accurately model the thermoelectric behavior, temperature dependent material properties are

implemented. Figure 4 illustrates the ZT and Seebeck coefficients' dependence on ambient temperature for p-type and n-type bismuth telluride.

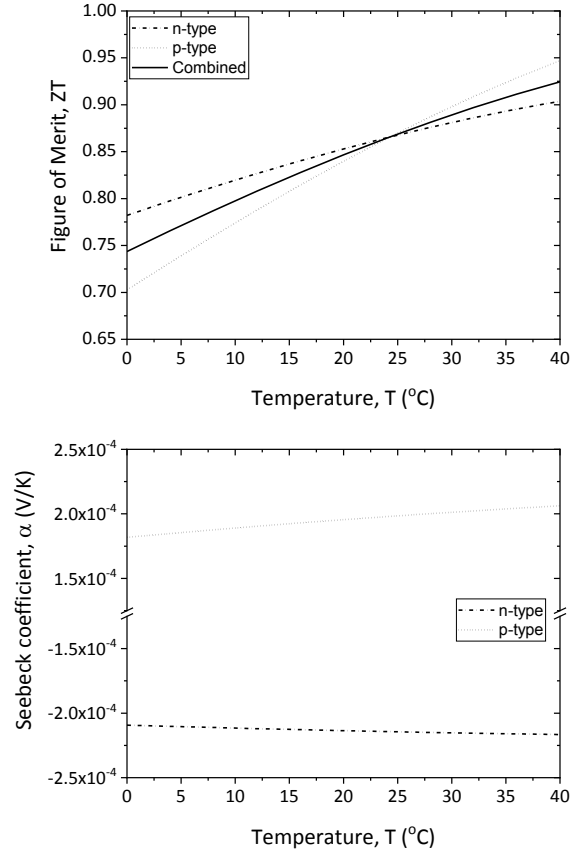


Figure 4: Temperature dependence of figure of merit (top) and Seebeck coefficients (bottom)

For the top and bottom plates of the TEG, ceramic aluminum oxide (96% purity) is used showing high electrical resistivity ($10^{14} \Omega \text{ m}$) and low thermal conductivity (25 W/(m K)). Interconnects between the p- and n-type semiconductors are made using copper with high thermal conductivity (400 W/(m K)) and low electrical resistivity ($1.68 \Omega \text{ m}$).

SIMULATION APPROACH AND RESULTS

We use steady state thermal-electric analysis in ANSYS Mechanical 18.2. The geometry model is based on commercially available thermoelectric modules from European thermoelectrics and Laird technologies. The simulations are carried out with top and bottom plates kept at a temperature difference of 1 K. The top face of the terminal thermocouple is electrically grounded. Table 1 comprises voltage output at open circuit conditions. The voltage obtained from the simulation results differ only slightly compared to the rated values. The voltage of a thermoelectric device scales with the number of thermocouples for a given temperature difference, while the power output depends upon the output voltage and the internal electrical resistance of the module.

Table 1: Comparison of manufacturer's data values with ANSYS model performance

					Manufacturer's data	ANSYS model		
Model	Dimensions (mm ³)	n	t_{TEG} (mm)	$A_{\text{Thermoleg}}$ (mm ²)	Rated voltage, V_{IK} (V)	Voltage, V_{IK} (V)	Power, P_{IK} (μW)	Power $_{\text{IK}}$ /Total area ($\mu\text{W}/\text{mm}^2$)
A ¹	40×40×6.8	324	3.8	1	0.05454	0.0667	95.85	0.2958
B ²	30×30×3.7	256	2.0	1	0.04781	0.0524	141.8	0.5538
C ³	23×23×3.6	144	2.1	0.960	-	0.0290	71.73	0.5186
D ⁴	25×25×3.4	256	2.06	0.672	-	0.0524	93.79	0.5448

^{1,2} GM250-161-12-40 and GM250-127-10-15 from European thermoelectrics (thermoelectric generators)

^{3,4} 926-1027-ND and 926-1015-ND from Laird technologies (thermoelectric coolers)

In turn, the electrical resistance of the module depends on the total device area, element length and material properties. To support geometry optimization of the TEG along with the implant assembly, power density provides a viable comparison parameter between the modules.

BIOHEAT MODELING

The thermoelectric modules discussed in the previous section were studied at a constant and uniform temperature difference of 1 K. To find an optimal power output for operation inside the human body and accurate *in silico* results, simulations of temperature distribution in human body are performed so as to identify locations with highest temperature gradient.

The human body is subject to the laws of thermodynamics, the food consumed is converted to bio-chemical energy, which among other things is used to maintain a body core temperature of about 37 °C (Parsons, 1993). The human body dissipates around 100 W at rest. The fat layer in the human body provides a thermal insulation, the largest temperature differences (typically 1-5 K) are found in the highest fat regions of the body (Chen, 2011). We consider the laws of thermodynamics to evaluate the temperature distribution in the human body, the heat-transfer processes are categorized into two categories: internal heat transfer and external heat transfer. Before considering the transient regulation effects, a steady-state simulation model is created in this work.

Internal Heat Transfer

To maintain the body core temperature, the body has to generate energy by processing the food ingested. Metabolism transforms the food into useable energy for the body and perfusion of blood allows the transport of heat throughout the body. Initially, we assume that the body's blood vessels have a fixed temperature of 37 °C and thereby neglect the blood circulation and direction of blood flow in the veins and arteries. The three main heat contributions for internal heat transfer are: conduction, metabolic heat generation and blood perfusion.

Heat conduction

Heat Conduction is the direct translation of heat energy, where heat flows from a hot body to a cold one. This heat flow is defined by the heat flux q_c . From the heat conduction equation (5), the heat flux is directly proportional to the temperature gradient, where the proportionality constant is a material parameter, the thermal conductivity κ .

$$q_c = -\kappa \frac{\partial T}{\partial x} \quad (5)$$

Metabolic Heat Generation

The human body will attempt to preserve or lose sufficient heat to the environment and try to maintain the body core temperature. For cells to perform the metabolic process, glucose and oxygen are required. They are transported to the individual cells through blood. This blood dependency connects the value for the metabolic heat generation directly with the blood perfusion. Since the simulation considers a steady state without blood flow, typical values for the metabolic heat for different tissues are assumed to be constant.

Blood Perfusion

Blood perfusion represents local blood flow through the capillary network and extracellular spaces in the tissue. The main blood vessels are the arteries and the veins. As these blood vessels reach the extremities of the body, many smaller blood vessels branch off to perfuse the organ, muscle, fat and skin tissue. In our model we assume stable one-directional blood flow resulting into constant values for blood perfusion for different types of tissues considered. The heat exchange between the blood and the perfused tissue is dependent on the local temperature T and the blood temperature T_{artery} , leading to a heating of the tissue. To characterize heat transfer in the tissues, the Pennes bioheat equation was used (Pennes, 1948):

$$\nabla \kappa \nabla T + Q_b + Q_m = \rho c \frac{\partial T}{\partial t} \quad (6)$$

The equation describes the influence of homogeneous distributed blood flow on the temperature distribution in

the tissue. where, $Q_b = \rho_b c_b \omega (T_{artery} - T(x, t))$; ρ , c , κ are the density, specific heat capacity and thermal conductivity of the tissue types ρ_b , c_b and ω are the density, specific heat and the perfusion rate of blood, κ is the thermal conductivity of the tissue and Q_m is the metabolic heat generation.

External Heat Transfer

The fact that the internal temperature is maintained at around 37 °C dictates that there is heat balance between the human body and its environment, the heat generated inside the human body should be balanced by the various heat losses due to convective, radiative and evaporative heat transfer. From a study (Gordon et al., 1976) related to model of temperature regulatory system the boundary condition at skin surface is described as:

$$-Ak \left. \frac{\partial T}{\partial r} \right|_s = h_c A_s (T_s - T_a) + \sigma \varepsilon F A (T_s^4 - T_r^4) + \dot{E}_s \quad (7)$$

From a computational fluid dynamic (CFD) study of combined simulation of airflow (Murakami, Kato and Zeng, 2000), the major contributions of heat loss were: radiation at about 38.1%, convective loss about 29% and evaporative heat loss of about 24.2%.

Radiation

The process of thermal radiation is described by the Stefan-Boltzmann law or black-body-radiation. As the human body (skin) is not a perfect black body, the emissivity parameter leads to a description of a grey body. The Stefan-Boltzmann law states:

$$Q_r = \sigma \varepsilon A_{skin} (T_{skin}^4 - T_r^4), \quad (8)$$

with the Stefan-Boltzmann constant σ , the skin surface area A_s and emissivity ε .

Convection

The skin tissue heats the local air through a continuous heat loss through convection as long as the ambient air temperature is below the skin surface temperature. The heat flux through convection is described by:

$$Q_b = h_c A_{skin} (T_{skin} - T_{ambient}), \quad (9)$$

where, h_c and A_s are the film coefficient and the skin surface area respectively.

SIMULATION AND RESULTS

The bioheat simulations are done for two different tissue geometries: Three layer simple cylindrical model and a tissue geometry obtained from magnetic resonance imaging (MRI) data.

MRI based Tissue Model – Thermal Simulation

The MRI human tissue model is obtained from the VHP-Female Version 2.2, which has been created using

the open-source high-resolution cryosection image dataset from the Visible Human Project®¹ of the U.S. National Library of Medicine. For the steady state thermal analysis in ANSYS Mechanical, we separated the right human forearm from the model and applied realistic tissue parameters available from the IT'IS database² such as specific heat, density, perfusion, metabolic heat generation rate (available in Table 2). Blood perfusion along with metabolic heat generation is applied to the muscle, fat and skin layers. The blood vessel bodies are set at a constant temperature of 37 °C. Additionally, the external heat transfer takes place to the environment at 12°C by means of radiation and convection applied to the skin surface, with a heat transfer coefficient of 3.1 W/(m² K) and emissivity of the body at 0.95.

Table 2: Material properties of various tissue types

Tissue type	Density ρ (kg/m ³)	Specific heat c (J/kgK)	Blood Perfusion ω (1/s)	Metabolic heat Q_m (W/m ³)
Muscle	1090.4	3421.2	6.67×10^{-4}	988.03
Fat	911	2348.3	4.96×10^{-4}	461.48
Skin	1109	3309.5	1.96×10^{-3}	1827.1

Figure 5 illustrates the temperature distribution across the human forearm. As no heat generation is applied to the bone, it remains cooler when compared to other tissues within the arm. Besides metabolic heat generation in muscle, fat and skin tissue heat is also originating from the blood vessels. Minimum temperature of around 26 °C is observed at the fingertips.

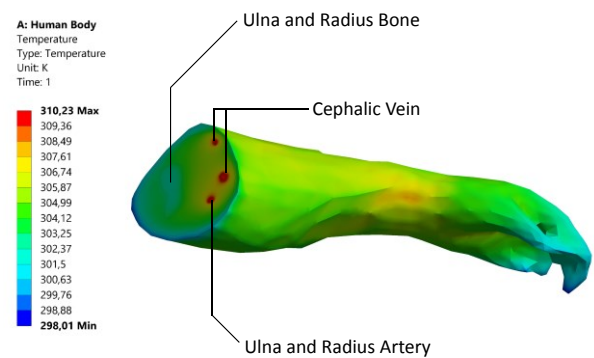


Figure 5: Temperature distribution across the human forearm

The maximum temperature in Figure 6 does not reach the temperature of the arterial blood, because the path does not cross any blood vessels. The temperature

¹https://www.nlm.nih.gov/research/visible/visible_human.html

²<https://www.itis.ethz.ch/virtual-population/tissue-properties/database/database-summary/>

decreases significantly across the fat tissue. The fat tissue has the lowest heat conduction property compared to other tissues. This leads to an isolating effect creating the largest temperature gradients.

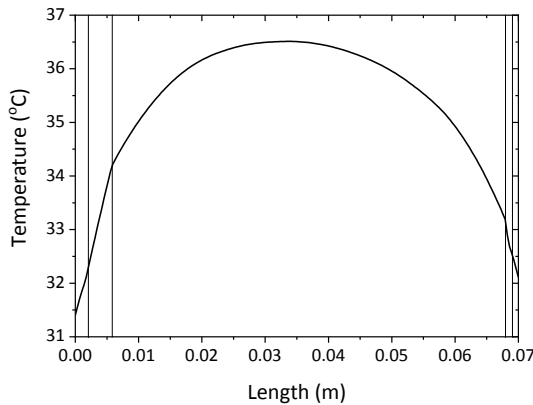


Figure 6: Temperature profile along a path through the forearm

Simplified Model – Fluid Simulation

A fluidic simulation considering heat transport from the fluid to the surrounding tissue overcomes the necessity to consider fixed temperatures of the blood inside the vessel structures. The fluidic model has been implemented in ANSYS FLUENT. The simulation domain is a concentric cylindrical tissue structure, comprised of three layers: muscle, subcutaneous fat and skin. Additionally, arteries and veins along with a simple bone are included to mimic the structure of a human forearm.

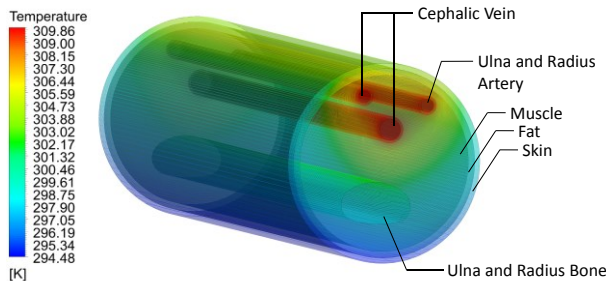


Figure 7: Temperature distribution in simplified geometry

An inlet temperature of 37 °C is applied to the arterial blood flowing with a velocity of 0.4 m/s, while the flow direction in the veins is considered in the opposite direction at 37 °C as there is a negligible drop in blood temperature. Individual metabolic heat generation rates are assigned to the various tissue types. The heat is dissipated by convection and radiation at the skin surface, with a heat transfer coefficient of 3.1 W/(m² K), emissivity of the body is set at 0.95 and the environmental temperature is set to 12 °C.

It can be observed from Figure 8, that the curve follows a similar trend when compared to Figure 6, which confirms that the maximum temperature drop occurs across the fat layer.

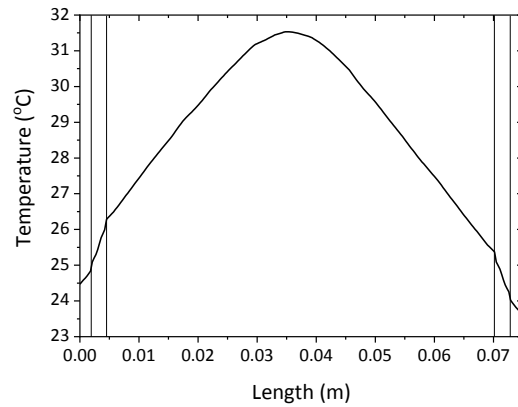


Figure 8: Temperature profile along a path through the simplified geometry

CONCLUSION AND FUTURE WORK

From the results, it is evident that the maximum temperature drop occurs across the fat layer. Thus the main task of further investigation is to integrate the thermoelectric generator into this human tissue region. Furthermore, as the heat transfer from human body is subject to variety of ambient changes throughout the day, we will study the thermoregulation response of the body in different environmental conditions

REFERENCES

- Amar, A., Kouki, A. and Cao, H. (2015). *Power Approaches for Implantable Medical Devices*. Sensors, 15(12), pp.28889-28914.
- Chen, A. (2011). *Thermal Energy Harvesting with Thermoelectrics for Self - powered Sensors: With Applications to Implantable Medical Devices, Body Sensor Networks and Aging in Place*. Ph.D. University of California, Berkeley.
- Gordon, R., Roemer, R. and Horvath, S. (1976). *A Mathematical Model of the Human Temperature Regulatory System - Transient Cold Exposure Response*. IEEE Transactions on Biomedical Engineering, BME-23(6), pp.434-444.
- Murakami, S., Kato, S. and Zeng, J. (2000). *Combined simulation of airflow, radiation and moisture transport for heat release from a human body*. Building and Environment, 35(6), pp.489-500.
- Parsonnet, V. and Cheema, A. (2003). *The Nature and Frequency of Postimplant Surgical Interventions: Pacing and Clinical Electrophysiology*, 26(12), pp.2308-2312.
- Pennes, H. (1948). *Analysis of Tissue and Arterial Blood Temperatures in the Resting Human Forearm*. Journal of Applied Physiology, 1(2), pp.93-122.
- Tritt, T. (2002). *Thermoelectric Materials: Principles, Structure, Properties, and Applications*. Encyclopedia of Materials: Science and Technology, pp.1-11.
- Watkins, C., Shen, B. and Venkatasubramanian, R. (2005). *Low-grade-heat energy harvesting using superlattice thermoelectrics for applications in implantable medical devices and sensors*. ICT 2005. 24th International Conference on Thermoelectrics, 2005.